

# Nuclear effects in charged-current quasielastic neutrino-nucleus scattering

**Maria B. Barbaro**

Università di Torino, Dipartimento di Fisica Teorica and INFN, Via P. Giuria 1, 10125 Torino, ITALY

E-mail: [barbaro@to.infn.it](mailto:barbaro@to.infn.it)

## Abstract.

After a short review of the recent developments in studies of neutrino-nucleus interactions, the predictions for double-differential and integrated charged current-induced quasielastic cross sections are presented within two different relativistic approaches: one is the so-called SuSA method, based on the superscaling behavior exhibited by electron scattering data; the other is a microscopic model based on relativistic mean field theory, and incorporating final-state interactions. The role played by the meson-exchange currents in the two-particle two-hole sector is explored and the results are compared with the recent MiniBooNE data.

## 1. Introduction

The analysis and interpretation of ongoing and future neutrino oscillation experiments strongly rely on the nuclear modeling for describing the interaction of neutrinos and anti-neutrinos with the detector. Moreover, neutrino-nucleus scattering has recently become a matter of debate in connection with the possibility of extracting information on the nucleon axial mass. Specifically, the data on muon neutrino charged-current quasielastic (CCQE) cross sections obtained by the MiniBooNE collaboration [1] are substantially underestimated by the Relativistic Fermi Gas (RFG) prediction. This has been ascribed either to effects in the elementary neutrino-nucleon interaction, or to nuclear effects. The most poorly known ingredient of the single nucleon cross section is the cutoff parameter  $M_A$  employed in the dipole prescription for the axial form factor of the nucleon, which can be extracted from  $\nu$  and  $\bar{\nu}$  scattering off hydrogen and deuterium and from charged pion electroproduction. If  $M_A$  is kept as a free parameter in the RFG calculation, a best fit of the MiniBooNE data yields a value of the order of  $1.35 \text{ GeV}/c^2$ , much larger than the average value  $M_A \simeq 1.026 \pm 0.021 \text{ GeV}/c^2$  extracted from the (anti)neutrino world data [2]. This should be taken more as an indication of incompleteness of the theoretical description of the data based upon the RFG, rather than as a true indication for a larger axial mass. Indeed it is well-known from comparisons with electron scattering data that the RFG model is too crude to account for the nuclear dynamics. Hence it is crucial to explore more sophisticated nuclear models before drawing conclusions on the value of  $M_A$ .

Several calculations have been recently performed and applied to neutrino reactions. These include, besides the approach that will be presented here, models based on nuclear spectral functions [3, 4, 5, 6, 7, 8, 9, 10], relativistic independent particle models [11, 12, 13], relativistic Green function approaches [14, 15, 16, 17, 18], models including NN correlations [19, 20, 21],

coupled-channel transport models [22, 23, 24, 25], RPA calculations [26, 27, 28] and models including multinucleon knock-out [29, 30, 31, 32]. The difference between the predictions of the above models can be large due to the different treatment of both initial and final state interactions. As a general trend, the models based on impulse approximation, where the neutrino is supposed to scatter off a single nucleon inside the nucleus, tend to underestimate the MiniBooNE data, while a sizable increase of the cross section is obtained when two-particle-two-hole (2p-2h) mechanisms are included in the calculations. Furthermore, a recent calculation performed within the relativistic Green function (RFG) framework has shown that at this kinematics the results strongly depend on the phenomenological optical potential used to describe the final state interaction between the ejected nucleon and the residual nucleus [18]. With an appropriate choice of the optical potential the RFG model can reproduce the MiniBooNE data without the need of modifying the axial mass (see Giusti’s contribution to this volume [33]).

The kinematics of the MiniBooNE experiment, where the neutrino flux spans a wide range of energies reaching values as high as 3 GeV, demands relativity as an essential ingredient. This is illustrated in Fig. 1, where the relativistic and non-relativistic Fermi gas results for the CCQE double differential cross section of 1 GeV muon neutrinos on  $^{12}\text{C}$  are shown as a function of the outgoing muon momentum and for two values of the muon scattering angle. The relativistic effects, which affect both the kinematics and the dynamics of the problem, have been shown to be relevant even at moderate momentum and energy transfers [34, 35]. Hence in our approach

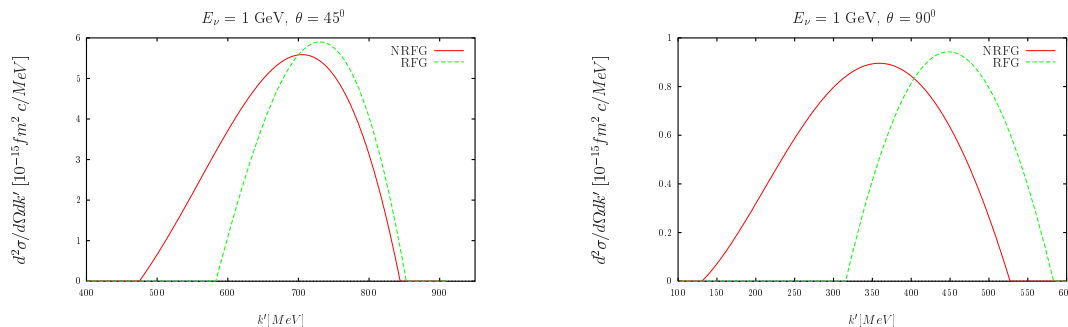


**Figure 1.**  $\nu_\mu$  CCQE double differential cross sections on  $^{12}\text{C}$  displayed versus the outgoing muon momentum for non-relativistic (NRFG) and relativistic (RFG) Fermi gas.

we try to retain as much as possible the relativistic aspects of the problems.

In spite of its simplicity, the RFG has the merit of incorporating an exact relativistic treatment, fulfilling the fundamental properties of Lorentz covariance and gauge invariance. However, it badly fails to reproduce the electron scattering data, in particular when it is compared with the Rosenbluth-separated longitudinal and transverse responses. Comparison with electron scattering data must be a guiding principle in selecting reliable models for neutrino reactions. A strong constraint in this connection is represented by the “superscaling” analysis of the world inclusive ( $e, e'$ ) data: in Refs. [36, 37, 38, 39, 40] it has been proved that, for sufficiently large momentum transfers, the reduced cross section (namely the double differential cross section divided by the appropriate single nucleon factors), when represented versus the scaling variable  $\psi$  [41], is largely independent of the momentum transfer (first-kind scaling) and of the nuclear target (second-kind scaling). The simultaneous occurrence of the two kinds of scaling is called superscaling. Moreover, from the experimental longitudinal response a phenomenological quasielastic scaling function has been extracted that shows a clear asymmetry with respect to the quasielastic peak (QEP) with a long tail extended to positive values of the scaling variable, i.e., larger energy transfers. On the contrary the RFG model, as well as

most models based on impulse approximation, give a symmetric superscaling function with a maximum value 20-30% higher than the data [42].

In this contribution, after recalling the basic formalism for CCQE reactions and their connection with electron scattering, we shall illustrate two models which provide good agreement with the above properties of electron scattering data: one of them, the relativistic mean field (RMF) model, comes from microscopic many-body theory, the other, the superscaling approximation (SuSA) model, is extracted from  $(e, e')$  phenomenology. We shall then include the contribution of 2p-2h excitations in the SuSA model and finally compare our results with the MiniBooNE double differential, single differential and total cross sections. Most of the results which will be presented are contained in Refs. [43] and [44].

## 2. Formalism

Charged current quasielastic muonic neutrino scattering  $(\nu_\mu, \mu^-)$  off nuclei is very closely related to quasielastic inclusive electron scattering  $(e, e')$ . However two major differences occur between the two processes:

- (i) in the former case the probe interacts with the nucleus via the weak force, in the latter the interaction is (dominantly) electromagnetic. While the weak vector current is related to the electromagnetic one via the CVC theorem, the axial current gives rise to a more complex structure of the cross sections, with new response functions which cannot be related to the electromagnetic ones. As a consequence, while in electron scattering the double-differential cross section can be expressed in terms of two response functions, longitudinal and transverse with respect to three-momentum carried by the virtual photon, for the CCQE process it can be written according to a Rosenbluth-like decomposition as [45]

$$\left[ \frac{d^2\sigma}{dT_\mu d\cos\theta} \right]_{E_\nu} = \sigma_0 \left[ \hat{V}_L R_L + \hat{V}_T R_T + \hat{V}_{T'} R_{T'} \right], \quad (1)$$

where  $T_\mu$  and  $\theta$  are the muon kinetic energy and scattering angle,  $E_\nu$  is the incident neutrino energy,  $\sigma_0$  is the elementary cross section,  $\hat{V}_i$  are kinematic factors and  $R_i$  are the nuclear response functions, the indices  $L, T, T'$  referring to longitudinal, transverse, transverse-axial, components of the nuclear current, respectively. The expression (1) is formally analogous to the inclusive electron scattering case, but: *i*) the “longitudinal” response  $R_L$  takes contributions from the charge (0) and longitudinal (3) components of the nuclear weak current, which, at variance with the electromagnetic case, are not related to each other by current conservation, *ii*)  $R_L$  and  $R_T$  have both “VV” and “AA” components (stemming from the product of two vector or axial currents, respectively), *iii*) a new response,  $R_{T'}$ , arises from the interference between the axial and vector parts of the weak nuclear current. In Fig. 2 we show the separate contributions of the three responses in (1), evaluated in the RFG model for the  $^{12}\text{C}$  target nucleus, for two different values of the scattering angle. It can be seen that in the forward direction the transverse response dominates over the longitudinal and transverse-axial ones, whereas at higher angles the  $L$ -component becomes negligible and the  $T'$  and  $T$  responses are almost equal. This cancellation has important consequences on antineutrino-nucleus scattering, where the response  $R_{T'}$  has opposite sign.

- (ii) In  $(e, e')$  experiments the energy of the electron is well-known, and therefore the detection of the outgoing electron univoquely determines the energy and momentum transferred to the nucleus. In neutrino experiments the neutrino energy is not known, but distributed over a range of values (for MiniBooNE from 0 to 3 GeV with an average value of about 0.8 GeV). The cross section must then be evaluated as an average over the experimental flux

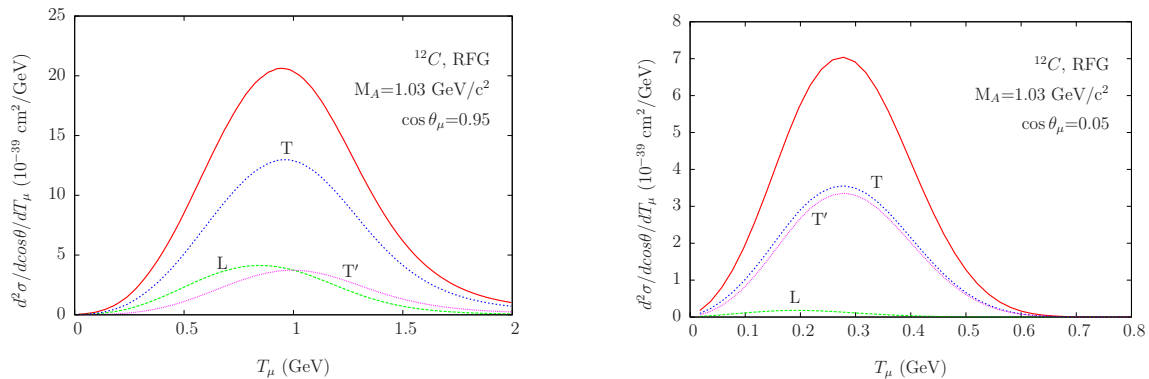


**Figure 2.** Separate contributions of the RFG longitudinal ( $L$ ), transverse ( $T$ ) and axial-vector interference ( $T'$ ) responses to the double differential  $\nu_\mu$ CCQE cross sections displayed versus the muon kinetic energy at two different angles. The neutrino energy is averaged over the MiniBooNE flux and the axial mass parameter has the standard value.

$\Phi(E_\nu)$

$$\frac{d^2\sigma}{dT_\mu d\cos\theta} = \frac{1}{\Phi_{tot}} \int \left[ \frac{d^2\sigma}{dT_\mu d\cos\theta} \right]_{E_\nu} \Phi(E_\nu) dE_\nu, \quad (2)$$

which may require to account for effects not included in models devised for quasi-free scattering. This is, for instance, the situation at the most forward scattering angles, where a significant contribution in the cross section comes from very low-lying excitations in nuclei [43], as illustrated in Fig. 3: here the double differential cross section is evaluated in the SuSA model (see later) at the MiniBooNE kinematics and the lowest angular bin and compared with the result obtained by excluding the energy transfers lower than 50 MeV from the flux-integral (2). It appears that at these angles 30-40% of the cross section

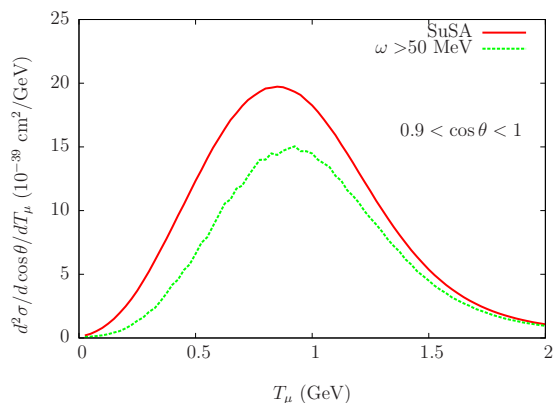


**Figure 3.** (Color online) Solid lines (red online): flux-integrated  $\nu_\mu$ CCQE cross sections on  $^{12}\text{C}$  calculated in the SuSA model for a specific bin of scattering angle. Dashed lines (green online): a lower cut  $\omega = 50$  MeV is set in the integral over the neutrino flux.

corresponds to very low energy transfers, where collective effects dominate. Moreover, processes involving meson exchange currents (MEC), which can excite both one-particle-one-hole (1p1h) and two-particle-two-hole (2p-2h) states via the exchange of a virtual meson, should also be taken into account, since they lead to final states where no pions are present, classified as “quasielastic” in the MiniBooNE experiment.

### 3. Models

In this Section we briefly outline the main ingredients of the RMF and SuSA model and we illustrate our calculation of the contribution of 2p-2h meson exchange currents.

### 3.1. RMF

In the RMF model a fully relativistic description of both the kinematics and the dynamics of the process is incorporated.

Details on the RMF model applied to inclusive QE electron and CCQE neutrino reactions can be found in Refs. [46, 47, 48, 49, 50, 51]. Here we simply recall that the weak response functions are given by taking the appropriate components of the weak hadronic tensor, constructed from the single-nucleon current matrix elements

$$\langle J_W^\mu \rangle = \int d\mathbf{r} \bar{\phi}_F(\mathbf{r}) \hat{J}_W^\mu(\mathbf{r}) \phi_B(\mathbf{r}), \quad (3)$$

where  $\phi_B$  and  $\phi_F$  are relativistic bound-state and scattering wave functions, respectively, and  $\hat{J}_W^\mu$  is the relativistic one-body current operator modeling the coupling between the virtual  $W$ -boson and a nucleon. The bound nucleon states are described as self-consistent Dirac-Hartree solutions, derived by using a Lagrangian containing  $\sigma$ ,  $\omega$  and  $\rho$  mesons [52, 53, 54]. The outgoing nucleon wave function is computed by using the same relativistic mean field (scalar and vector energy-independent potentials) employed in the initial state and incorporates the final state interactions (FSI) between the ejected proton and the residual nucleus.

The RMF model successfully reproduces the scaling behaviour of inclusive QE ( $e, e'$ ) processes and, more importantly, it gives rise to a superscaling function with a significant asymmetry, namely, in complete accord with data [46, 47]. This is a peculiar property associated to the consistent treatment of initial and final state interactions. It has been shown in Refs. [46, 47] that other versions of the RMF model, which deal with the FSI through a real relativistic optical potential, are not capable of reproducing the asymmetry of the scaling function.

Moreover, contrary to most other models based on impulse approximation, where scaling of the zeroth kind - namely the equality of the longitudinal and transverse scaling functions - occurs, the RMF model provides  $L$  and  $T$  scaling functions which differ by typically 20%, the  $T$  one being larger. This agrees with the analysis [39] of the existing  $L/T$  separated data, which has shown that, after removing inelastic contributions and two-particle-emission effects, the purely nucleonic transverse scaling function is significantly larger than the longitudinal one.

### 3.2. SuSA

The SuSA model is based on the phenomenological superscaling function extracted from the world data on quasielastic electron scattering [37]. The model has been extended to the  $\Delta$ -resonance region in Ref. [45] and to neutral current scattering in Ref. [55], but here we restrict our attention to the quasielastic charged current case.

Assuming the scaling function  $f$  extracted from ( $e, e'$ ) data to be universal, i.e., valid for electromagnetic and weak interactions, in [45, 56] CCQE neutrino-nucleus cross sections have been evaluated by multiplying  $f$  by the corresponding elementary weak cross section. Thus in the SuSA approach all the nuclear responses in (1) are expressed as follows

$$R_K = N \frac{2E_F}{k_F q} U_K(q, \omega) f(\psi) \quad , \quad (K = L, T, T') \quad (4)$$

where  $U_K$  are the elementary lepton-nucleon responses,  $E_F$  and  $k_F$  are the Fermi energy and momentum,  $N$  is the number of nucleons (neutrons in the  $\nu_\mu$  CCQE case) and  $f(\psi)$  in the universal superscaling function, depending only on the scaling variable  $\psi$  [41].

The SuSA approach provides nuclear-model-independent neutrino-nucleus cross sections and reproduces the longitudinal electron data by construction. However, its reliability rests on some basic assumptions.

First, it assumes that the scaling function - extracted from *longitudinal* ( $e, e'$ ) data - is appropriate for all of the weak responses involved in neutrino scattering (charge-charge, charge-longitudinal, longitudinal-longitudinal, transverse and axial), and is independent of the vector or axial nature of the nuclear current entering the hadronic tensor. In particular it assumes the equality of the longitudinal and transverse scaling functions (scaling of the zeroth kind), which, as mentioned before, has been shown to be violated both by experiment and by some microscopic models, for example relativistic mean field theory.

Second, the charged-current neutrino responses are purely isovector, whereas the electromagnetic ones contain both isoscalar and isovector components and the former involve axial-vector as well as vector responses. One then has to invoke a further kind of scaling, namely the independence of the scaling function of the choice of isospin channel — so-called scaling of the third kind.

Finally, the SuSA approach neglects violations of scaling of first and second kinds. These are known to be important at energies above the QE peak and to reside mainly in the transverse channel, being associated to effects which go beyond the impulse approximation: inelastic scattering, meson-exchange currents and the associated correlations needed to conserve the vector current. The inclusion of these contributions in the SuSA model is discussed in the next paragraph.

### 3.3. $2p$ - $2h$ MEC

Meson exchange currents are two-body currents carried by a virtual meson which is exchanged between two nucleons in the nucleus. They are represented by the diagrams in Fig. 4, where the external lines correspond to the virtual boson ( $\gamma$  or  $W$ ) and the dashed lines to the exchanged meson: in our approach we only consider the pion, which is believed to give the dominant contribution in the quasielastic regime. The thick lines in diagrams (d)-(g) represent the propagation of a  $\Delta$ -resonance. The explicit relativistic expressions for the current matrix elements can be found, e.g., in Ref. [57].

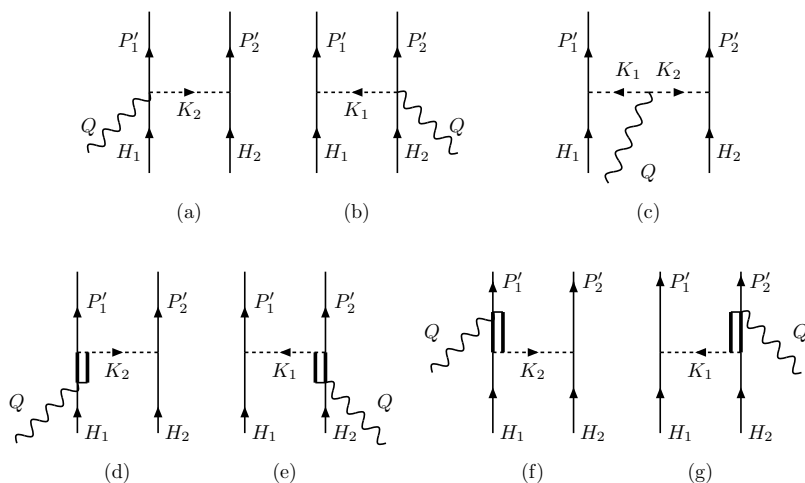


**Figure 4.** Two-body meson-exchange currents. (a) and (b): “contact”, or “seagull” diagram; (c): “pion-in-flight” diagram; (d)-(g): “ $\Delta$ -MEC” diagram.

Being two-body currents, the MEC can excite both one-particle one-hole (1p-1h) and two-particle two-hole (2p-2h) states. In the 1p-1h sector, MEC studies of electromagnetic ( $e, e'$ ) process have been performed for low-to-intermediate momentum transfers (see, e.g., [58, 35, 59, 60]), showing a small reduction of the total response at the quasielastic peak, mainly due to diagrams involving the electroexcitation of the  $\Delta$  resonance.

However in a perturbative scheme where all the diagrams containing one and only one pionic line are retained, the MEC are not the only diagrams arising, but pionic correlation contributions, where the virtual boson is attached to one of the two interacting nucleons, should also be considered. These are represented by the same diagrams as in Fig. 4(d)-(g), where now the thick lines are nucleon propagators. Only when all the diagrams are taken into account gauge invariance is fulfilled and the full two-body current is conserved. Correlation diagrams have been shown to roughly compensate the pure MEC contribution [58, 35, 59, 60], so that in first approximation we can neglect the 1p-1h sector and restrict our attention to 2p-2h final states.

The contribution to the inclusive electron scattering cross section arising from two-nucleon emission via meson exchange current interactions was first calculated in the Fermi gas model in Refs. [61, 62], where sizable effects were found at large energy transfers. In these references a non-relativistic reduction of the currents was performed, while fully relativistic calculations have been developed more recently in Refs. [63, 64, 57]. It has been found that the MEC give a significant positive contribution which leads to a partial filling of the “dip” between the quasielastic peak and the analogous peak associated with the excitation of the  $\Delta$  resonance. Moreover, the MEC have been shown to break scaling of both first and second kinds [65].

Here we use the fully relativistic model of [64], where all the MEC many-body diagrams containing two pionic lines that contribute to the electromagnetic 2p-2h transverse response were taken into account. Similar results for the 2p-2h MEC were obtained in Ref. [57], where the correlation diagrams were also included.

In order to apply the model to neutrino scattering, we observe that in lowest order the 2p2h sector is not directly reachable for the axial-vector matrix elements. Hence the MEC affect only the transverse polar vector response,  $R_T^{VV}$ . Note that, at variance with the 1p-1h sector, where the contribution of the MEC diagrams originates from the interference between 1-body and 2-body amplitudes and has therefore no definite sign (in fact it turns out to be negative due to the dominance of the diagrams involving the  $\Delta$ ), the 2p-2h contribution of MEC to the nuclear responses is the square of an amplitude, hence it is positive by definition. Therefore the net effect of 2p-2h MEC to neutrino scattering is to increase the transverse vector response function, as will be illustrated in the next section.

#### 4. Results

In this Section we present the predictions of the above models and their comparison with the MiniBooNE data. More results can be found in Refs. [43] and [44].

In Figs. 5 and 6 the flux-integrated double-differential cross section per target nucleon for the  $\nu_\mu$ CCQE process on  $^{12}\text{C}$  is evaluated for the three nuclear models above described: the RMF model and the SuSA approach with and without the contribution of 2p-2h MEC. In Fig. 5 the cross sections are displayed versus the muon kinetic energy  $T_\mu$  at fixed scattering energy  $\theta$ , in Fig. 6 they are displayed versus  $\cos\theta$  at fixed  $T_\mu$ .

It appears that the SuSA predictions systematically underestimate the experimental cross section, the discrepancy being larger at high scattering angle and low muon kinetic energy. The inclusion of 2p-2h MEC tends to improve the agreement with the data at low angles, but it is not sufficient to account for the discrepancy at higher angles. The RMF calculation, which, as already mentioned, incorporates violations of scaling of the zeroth kind with a substantial enhancement of the vector transverse response, yields cross sections which are in general larger than the SuSA ones. In particular, in the region close to the peak in the cross section, the RMF result becomes larger than the one obtained with SuSA+MEC. Furthermore, the RMF does better than SuSA in fitting the shape of the experimental curves versus both the scattering angle and the muon energy: this is partly due to the fact that the RMF is better describing the low-energy excitation region whereas the SuSA model has no predictive power at very low angles, where the cross section is dominated by low excitation energies and the superscaling

ideas are not supposed to apply.

Concerning the SuSA+MEC results, a possible explanation of the theory/data disagreement is the fact that, as already mentioned, a fully consistent treatment of two-body currents should take into account not only the genuine MEC contributions, but also the correlation diagrams that are necessary in order to preserve the gauge invariance of the theory. This, however, is not an easy task because in an infinite system like the RFG the correlation diagrams give rise to divergences which need to be regularized [57]. The divergences arise from a double pole in some of the diagrams, associated to the presence of on-shell nucleon propagators. Different prescriptions have been used in the literature in order to overcome this problem [66, 67, 68, 57], leading to a substantial model-dependence of the results. In particular in Ref. [57] the divergence has been cured by introducing a parameter  $\epsilon$  which accounts for the finite size of the nucleus (and therefore the finite time of propagation of a nucleon inside the nucleus) and the  $\epsilon$ -dependence of the contribution of correlation diagrams has been explored. The study has shown that for reasonable values of the parameter the correlations add to the pure MEC in the high-energy tail and are roughly of the same order of magnitude, but now contributing to both the longitudinal and the transverse channels. The inclusion of these terms in neutrino reactions is in progress [69] and is expected to give a further enhancement of the cross sections.

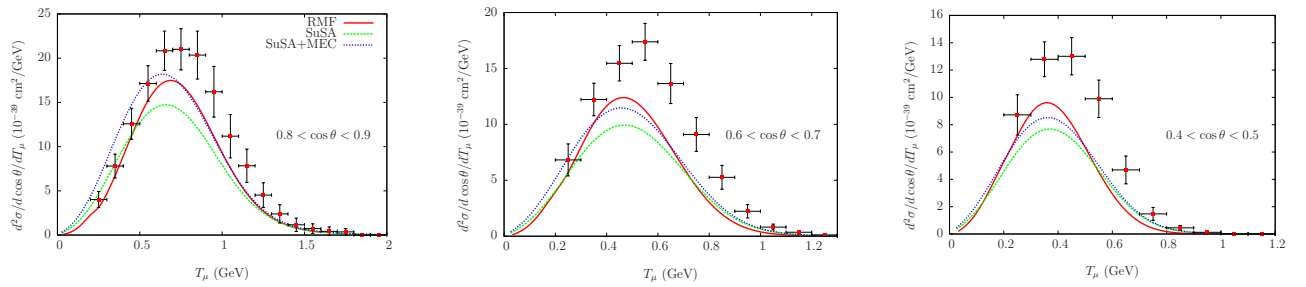


**Figure 5.** Flux-integrated double-differential cross section per target nucleon for the  $\nu_\mu$  CCQE process on  $^{12}\text{C}$  evaluated in the RMF (red) model and in the SuSA approach with (blue line) and without (green line) the contribution of MEC and displayed versus the muon kinetic energy  $T_\mu$  for three specific bins of the scattering angle. The data are from MiniBooNE [1].

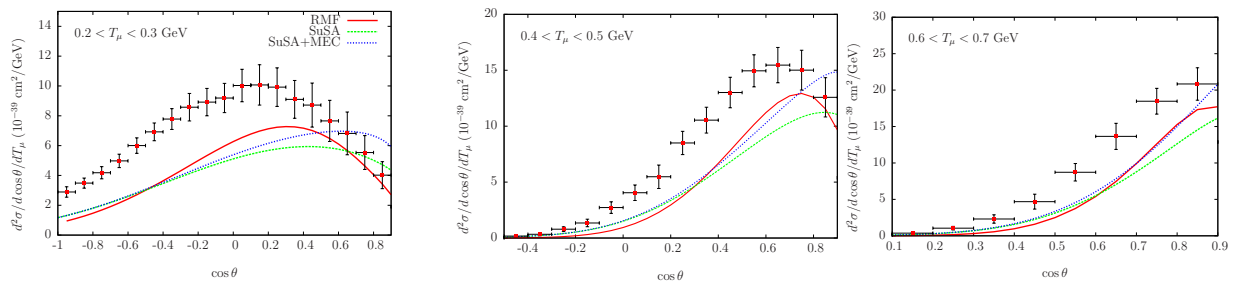


**Figure 6.** Flux-integrated double-differential cross section per target nucleon for the  $\nu_\mu$  CCQE process on  $^{12}\text{C}$  evaluated in the RMF (red) model and in the SuSA approach with (blue line) and without (green line) the contribution of MEC and displayed versus the muon scattering angle for three bins of the muon kinetic energy  $T_\mu$ . The data are from MiniBooNE [1].

The single differential cross sections with respect to the muon kinetic energy and scattering angle, respectively, are presented in Figs. 7 and 8, where the relativistic Fermi gas result is also shown for comparison: again it appears that the RMF gives slightly higher cross sections



than SuSA, due to the  $L/T$  unbalance, but both models still underestimate the data for most kinematics. The inclusion of 2p-2h excitations leads to a good agreement with the data at high  $T_\mu$ , but strength is still missing at the lower muon kinetic energies (namely higher energy transfers) and higher angles.

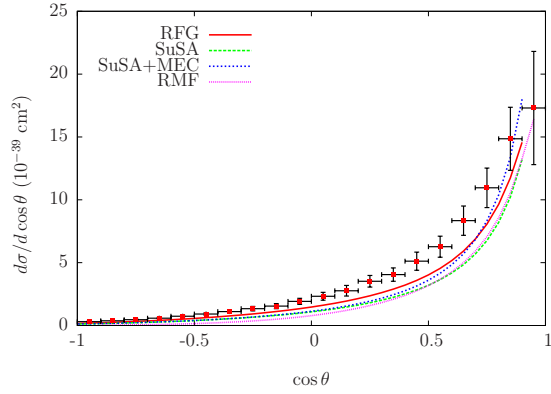


**Figure 7.** (Color online) Flux-averaged  $\nu_\mu$  CCQE cross section on  $^{12}\text{C}$  integrated over the scattering angle and displayed versus the muon kinetic energy. The data are from MiniBooNE [1].

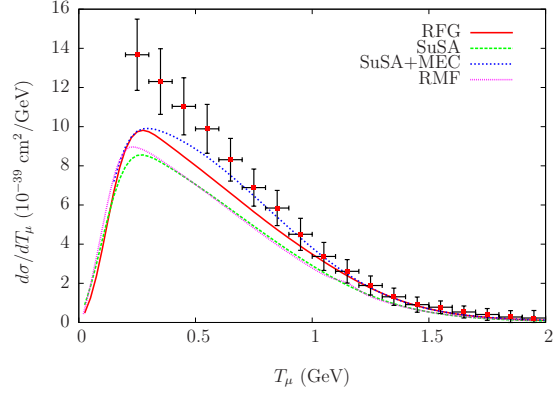


**Figure 8.** (Color online) Flux-averaged  $\nu_\mu$  CCQE cross section on  $^{12}\text{C}$  integrated over the muon kinetic energy and displayed versus the scattering angle. The data are from MiniBooNE [1].

Finally, in Fig. 9 the total (namely integrated over over all muon scattering angles and energies) CCQE cross section per neutron is displayed versus the neutrino energy and compared with the experimental flux-unfolded data. Besides the models above discussed, we show for comparison also the results of the relativistic mean field model when the final state interactions are ignored (denoted as RPWIA - relativistic plane wave impulse approximation) or described through a real optical potential (denoted as rROP). Note that the discrepancies between the various models, observed in Figs. 5 and 6, tend to be washed out by the integration, yielding very similar results for the models that include FSI (SuSA, RMF and rROP), all of them giving a lower total cross section than the models without FSI (RFG and RPWIA). On the other hand the SuSA+MEC curve, while being closer to the data at high neutrino energies, has a somewhat different shape with respect to the other models, in qualitative agreement with the relativistic calculation of [31]. It should be noted, however, that the result is affected by an uncertainty of about 5% associated with the treatment of the 2p-2h contribution at low momentum transfers and that pionic correlations are not included.

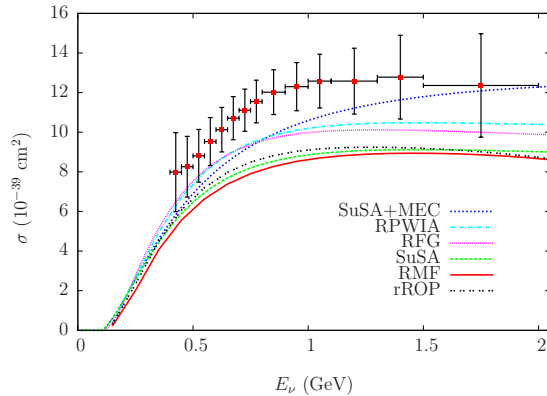


**Figure 9.** (Color online) Total CCQE cross section per neutron versus the neutrino energy. The curves corresponding to different nuclear models are compared with the flux unfolded MiniBooNE data [1].

## 5. Conclusions

Two different relativistic models, one (SuSA) phenomenological and the other (RMF) microscopic, have been applied to the study of charged-current quasielastic neutrino scattering and the impact of 2p-2h meson exchange currents on the cross sections has been investigated. The results can be summarized as follows:

- (i) Both the SuSA and the RMF models, in contrast with the relativistic Fermi gas, are fitting with good accuracy the longitudinal quasielastic electron scattering response at intermediate to high energy and momentum transfer.  
The SuSA and RMF models give very similar results for the integrated neutrino cross section and both substantially under-predict the MiniBooNE experimental data. However the comparison with the double differential experimental cross section reveals some differences between the two models, which are washed out by the integration. Indeed the RMF, although being lower than the data, reproduces better the slopes of the cross section versus the muon energy and scattering angle. This is essentially due to the enhancement of the transverse response, which arises from the self-consistent mean field approach of RMF (in particular from the consistent treatment of initial and final state interactions) and is absent in the superscaling approach.
- (ii) In relativistic or semi-relativistic models final state interactions have been shown to play an essential role for reproducing the shape and size of the electromagnetic response [50, 46, 51] and cannot be neglected, in our scheme, in the study of neutrino interactions. The effect of final state interactions in the SuSA and RMF models is to lower the cross section, giving a discrepancy with the data larger than the RFG.
- (iii) In the transverse channel, the analysis of  $(e, e')$  data points to the importance of meson-exchange currents which, through the excitation of two-particle-two-hole states, are partially responsible of filling the “dip” region between the QE and  $\Delta$  peaks. The 2p-2h MEC can be even more relevant in the CCQE process, where “quasielastic” implies simply that no pions are present in the final state but, due to the large energy region spanned by the neutrino flux, processes involving the exchange of virtual pions can give a sizable contribution. In fact the inclusion of 2p-2h MEC contributions yields larger cross sections and accordingly better agreement with the data, although the theoretical curves still lie below the data at high angles and low muon energy. It should be stressed, however, that the present calculation, though exact and fully relativistic, is incomplete. In order to preserve gauge invariance the full two-body current, including not only the MEC but also the corresponding correlation diagrams, must be included. These have recently been shown to yield a sizable contribution at high energies in  $(e, e')$  scattering [57] and are likely to improve the agreement of our models with the MiniBooNE data.
- (iv) In all our calculations the standard value  $M_A = 1.03 \text{ GeV}/c^2$  has been used. It has been suggested that a larger value of the axial mass ( $1.35 \text{ GeV}/c^2$ ) would eliminate the disagreement with the data. However the fit was done using a RFG analysis, and more sophisticated nuclear models must be explored before drawing conclusions on the actual value of the axial mass. For instance in Ref. [70] it is shown that the MiniBooNE data can as well be fitted by effectively incorporating some nuclear effects in the magnetic form factor of the bound nucleon, without changing the axial mass.

Although our scope here is not to extract a value for the axial mass of the nucleon, but rather to understand which nuclear effects are effectively accounted for by a large axial cutoff parameter, let us mention that a best fit of the RMF and SuSA results to the MiniBooNE experimental cross section gives an effective axial mass  $M_A^{\text{eff}} \simeq 1.5 \text{ GeV}/c^2$  and values in the range  $1.35 < M_A^{\text{eff}} < 1.65 \text{ GeV}/c^2$  yield results compatible with the MiniBooNE data within the experimental errors. A similar analysis in the model including the 2p-2h contribution

will be possible only when the above mentioned correlation diagrams will be consistently evaluated [69].

## Acknowledgments

I would like to thank J.E. Amaro, J.A. Caballero, T.W. Donnelly, J.M. Udias and C.W. Williamson for the fruitful collaboration which lead to the results reported in this contribution.

## References

- [1] A. A. Aguilar-Arevalo *et al.* [MiniBooNE Collaboration], Phys. Rev. D **81**, 092005 (2010).
- [2] V. Bernard, L. Elouadrhiri and U. G. Meissner, J. Phys. G **28**, R1 (2002).
- [3] M. B. Barbaro, A. De Pace, T. W. Donnelly, A. Molinari and M. J. Musolf, Phys. Rev. C **54**, 1954 (1996).
- [4] O. Benhar, N. Farina, H. Nakamura, M. Sakuda and R. Seki, Phys. Rev. D **72**, 053005 (2005).
- [5] O. Benhar and D. Meloni, Nucl. Phys. A **789**, 379 (2007).
- [6] O. Benhar and D. Meloni, Phys. Rev. D **80**, 073003 (2009).
- [7] A. M. Ankowski, O. Benhar and N. Farina, Phys. Rev. D **82**, 013002 (2010).
- [8] O. Benhar, P. Coletti and D. Meloni, Phys. Rev. Lett. **105**, 132301 (2010).
- [9] C. Juszczak, J. T. Sobczyk and J. Zmuda, Phys. Rev. C **82**, 045502 (2010).
- [10] A. M. Ankowski and O. Benhar, Phys. Rev. C **83**, 054616 (2011).
- [11] W. M. Alberico *et al.*, Nucl. Phys. A **623**, 471 (1997).
- [12] W. M. Alberico *et al.*, Phys. Lett. B **438**, 9 (1998).
- [13] W. M. Alberico *et al.*, Nucl. Phys. A **651**, 277 (1999).
- [14] A. Meucci, C. Giusti and F. D. Pacati, Nucl. Phys. A **739**, 277 (2004).
- [15] A. Meucci, C. Giusti and F. D. Pacati, Nucl. Phys. A **744**, 307 (2004).
- [16] A. Meucci, C. Giusti and F. D. Pacati, Nucl. Phys. A **773**, 250 (2006).
- [17] A. Meucci, J. A. Caballero, C. Giusti and J. M. Udias, Phys. Rev. C **83**, 064614 (2011).
- [18] A. Meucci, M. B. Barbaro, J. A. Caballero, C. Giusti and J. M. Udias, arXiv:1107.5145 [nucl-th].
- [19] A. N. Antonov *et al.*, Phys. Rev. C **74**, 054603 (2006).
- [20] A. N. Antonov, M. V. Ivanov, M. B. Barbaro, J. A. Caballero, E. Moya de Guerra and M. K. Gaidarov, Phys. Rev. C **75**, 064617 (2007).
- [21] M. V. Ivanov, M. B. Barbaro, J. A. Caballero, A. N. Antonov, E. Moya de Guerra and M. K. Gaidarov, Phys. Rev. C **77**, 034612 (2008).
- [22] T. Leitner, L. Alvarez-Ruso and U. Mosel, Phys. Rev. C **73**, 065502 (2006).
- [23] T. Leitner, L. Alvarez-Ruso and U. Mosel, Phys. Rev. C **74**, 065502 (2006).
- [24] O. Buss, T. Leitner, U. Mosel and L. Alvarez-Ruso, Phys. Rev. C **76**, 035502 (2007).
- [25] T. Leitner and U. Mosel, Phys. Rev. C **81**, 064614 (2010).
- [26] J. Nieves, J. E. Amaro and M. Valverde, Phys. Rev. C **70**, 055503 (2004) [Erratum-ibid. C **72**, 019902 (2005)].
- [27] J. Nieves, M. Valverde and M. J. Vicente Vacas, Phys. Rev. C **73**, 025504 (2006).
- [28] M. Valverde, J. E. Amaro and J. Nieves, Phys. Lett. B **638**, 325 (2006).
- [29] M. Martini, M. Ericson, G. Chanfray and J. Marteau, Phys. Rev. C **80**, 065501 (2009).
- [30] M. Martini, M. Ericson, G. Chanfray and J. Marteau, Phys. Rev. C **81**, 045502 (2010).
- [31] J. Nieves, I. Ruiz Simo and M. J. Vicente Vacas, Phys. Rev. C **83**, 045501 (2011).
- [32] J. Nieves, I. R. Simo and M. J. V. Vacas, arXiv:1106.5374 [hep-ph].
- [33] C. Giusti and A. Meucci, arXiv:1107.5425 [nucl-th].
- [34] J. E. Amaro, M. B. Barbaro, J. A. Caballero, T. W. Donnelly and A. Molinari, Nucl. Phys. A **643**, 349 (1998).
- [35] J. E. Amaro, M. B. Barbaro, J. A. Caballero, T. W. Donnelly and A. Molinari, Phys. Rept. **368**, 317 (2002).
- [36] D. B. Day, J. S. McCarthy, T. W. Donnelly and I. Sick, Ann. Rev. Nucl. Part. Sci. **40**, 357 (1990).
- [37] J. Jourdan, Nucl. Phys. A **603** (1996) 117.
- [38] T. W. Donnelly and I. Sick, Phys. Rev. Lett. **82**, 3212 (1999).
- [39] T. W. Donnelly and I. Sick, Phys. Rev. C **60**, 065502 (1999).
- [40] C. Maieron, T. W. Donnelly and I. Sick, Phys. Rev. C **65** (2002) 025502.
- [41] W. M. Alberico, A. Molinari, T. W. Donnelly, E. L. Kronenberg and J. W. Van Orden, Phys. Rev. C **38**, 1801 (1988).
- [42] M. B. Barbaro, J. E. Amaro, J. A. Caballero, T. W. Donnelly, Proceedings of the XXV International Workshop on Nuclear Theory, Rila, 2005, "Nuclear Theory 25", Ed. S. Dimitrova, Heron Press, Sofia, 2006; [arXiv:nucl-th/0609057].

- [43] J. E. Amaro, M. B. Barbaro, J. A. Caballero, T. W. Donnelly and C. F. Williamson, *Phys. Lett. B* **696**, 151 (2011).
- [44] J. E. Amaro, M. B. Barbaro, J. A. Caballero, T. W. Donnelly and J. M. Udias, *Phys. Rev. D* **84**, 033004 (2011).
- [45] J. E. Amaro, M. B. Barbaro, J. A. Caballero, T. W. Donnelly, A. Molinari and I. Sick, *Phys. Rev. C* **71** (2005) 015501.
- [46] J. A. Caballero, *Phys. Rev. C* **74**, 015502 (2006).
- [47] J. A. Caballero, J. E. Amaro, M. B. Barbaro, T. W. Donnelly and J. M. Udias, *Phys. Lett. B* **653**, 366 (2007).
- [48] J. A. Caballero, J. E. Amaro, M. B. Barbaro, T. W. Donnelly, C. Maieron and J. M. Udias, *Phys. Rev. Lett.* **95**, 252502 (2005).
- [49] J. E. Amaro, M. B. Barbaro, J. A. Caballero and T. W. Donnelly, *Phys. Rev. Lett.* **98** (2007) 242501.
- [50] C. Maieron, M. C. Martinez, J. A. Caballero and J. M. Udias, *Phys. Rev. C* **68**, 048501 (2003).
- [51] J. E. Amaro, M. B. Barbaro, J. A. Caballero, T. W. Donnelly and J. M. Udias, *Phys. Rev. C* **75**, 034613 (2007).
- [52] C. J. Horowitz, B. D. Serot, *Nucl. Phys. A* **368**, 503 (1981); *Phys. Lett. B* **86**, 146 (1979).
- [53] B. D. Serot, J. D. Walecka, *Adv. Nucl. Phys.* **16**, 1. Eds. J. W. Negele, E. W. Vogt. Plenum Press, New York (1986).
- [54] M. M. Sharma, M. A. Nagarajan and P. Ring, *Phys. Lett. B* **312**, 377 (1993).
- [55] J. E. Amaro, M. B. Barbaro, J. A. Caballero and T. W. Donnelly, *Phys. Rev. C* **73**, 035503 (2006).
- [56] J. E. Amaro, M. B. Barbaro, J. A. Caballero, T. W. Donnelly and C. Maieron, *Phys. Rev. C* **71**, 065501 (2005).
- [57] J. E. Amaro, C. Maieron, M. B. Barbaro, J. A. Caballero and T. W. Donnelly, *Phys. Rev. C* **82**, 044601 (2010).
- [58] W. M. Alberico, T. W. Donnelly and A. Molinari, *Nucl. Phys. A* **512**, 541 (1990).
- [59] J. E. Amaro, M. B. Barbaro, J. A. Caballero, T. W. Donnelly and A. Molinari, *Nucl. Phys. A* **723**, 181 (2003).
- [60] J. E. Amaro, M. B. Barbaro, J. A. Caballero, T. W. Donnelly, C. Maieron and J. M. Udias, *Phys. Rev. C* **81** (2010) 014606.
- [61] T. W. Donnelly, J. W. Van Orden, T. . J. De Forest and W. C. Hermans, *Phys. Lett. B* **76**, 393 (1978).
- [62] J. W. Van Orden and T. W. Donnelly, *Annals Phys.* **131** (1981) 451.
- [63] M. J. Dekker, P. J. Brussaard and J. A. Tjon, *Phys. Rev. C* **49**, 2650 (1994).
- [64] A. De Pace, M. Nardi, W. M. Alberico, T. W. Donnelly and A. Molinari, *Nucl. Phys. A* **726**, 303 (2003).
- [65] A. De Pace, M. Nardi, W. M. Alberico, T. W. Donnelly and A. Molinari, *Nucl. Phys. A* **741**, 249 (2004).
- [66] W. M. Alberico, M. Ericson and A. Molinari, *Annals Phys.* **154**, 356 (1984).
- [67] W. M. Alberico, A. De Pace, A. Drago and A. Molinari, *Riv. Nuovo Cim.* **14N5**, 1 (1991).
- [68] A. Gil, J. Nieves and E. Oset, *Nucl. Phys. A* **627**, 543 (1997).
- [69] J. E. Amaro et al., work in progress.
- [70] A. Bodek, H. Budd, E. Christy, arXiv:1106.0340 [hep-ph].